https://doi.org/10.5194/hess-2020-161
Preprint. Discussion started: 4 May 2020

Hydrology and Earth System Sciences
Discussions

Estimation of evapotranspiration through an improved daily global solar radiation in SEBAL model: a case study of the middle Heihe River Basin

Jingqiu Yin[1], Xinfa Qiu[1], Shoubo Li[1], Guoping Shi[1], Huiyu Liu[2]

[1]College of Geography Science, Nanjing University of Information Science & Technology, Nanjing, China

[2]College of Geography Science,Nanjing Normal University,Nanjing,China

Correspondence to: Jingqiu Yin (autumn4001@126.com)

Abstract: The agricultural activities, hydrologic cycle, and ecological environment are seriously influenced by evapotranspiration (ET), especially in arid and semi-arid areas. A new method for estimating daily global solar radiation (GSR) over rugged terrains in the middle Heihe River Basin is developed on the basis of Iqbal model C. And with the land surface parameters retrieved from multisource remote sensing data, a daily surface ET on June 21–24, 2009, is simulated by using surface energy balance algorithm for land (SEBAL) model. The results show:

1. An improved daily GSR with a resolution of 100 m×100 m is implemented. The mean absolute bias error (MABE) is 9 W/m^2, and the mean absolute relative bias error (MARBE) is 2.5%. The MABE of the daily GSR using the SEBAL model is 122.2 W/m^2, and the MARBE is 33.9%.

2. The spatial distribution of the daily GSR is more reasonable using the improved model than the original model. The GSR is larger on a sunny slope (an open place) than on a shady slope (a rugged place).

3. Bringing the new model into SEBAL significantly improves the accuracy of the ET. The MABE of ET decreases from 2.1 mm (original scheme) to 0.6 mm (improved scheme),

https://doi.org/10.5194/hess-2020-161
Preprint. Discussion started: 4 May 2020

and the MARBE declines from 44% to 13% accordingly. Moreover, the spatiotemporal resolution of the ET simulation is effectively improved by the combined moderate-resolution imaging spectroradiometer and thematic mapper surface parameters.

4. All highest ET value appeared in all types of water bodies, followed by farmland, forest, wetland, and residential areas, the lowest values appeared over bare rock land. The water consumption in these areas is dominated by agriculture. The new results provide better theoretical basis and scientific guidance for ecosystem protection and sustainable utilization of water resources.

1. Introduction

About 60% of global precipitation is consumed by evapotranspiration (ET), while 99% of water in farmland system is consumed by ET (Kit, 2000). As an important part of water cycle, ET is of great significance for understanding the water cycle process, regulating the hydrological process by vegetation, and rational utilization of limited water resources (Sellers et al., 1996), especially in arid and semi-arid areas. Therefore, the accurate determination and estimation of the daily ET can satisfy the requirements of not only agricultural production but also other ecological water requirements and provide scientific guidance for the rational utilization and distribution of water resources (Nie et al., 2004; Rahman et al., 2016), especially during the growing season when numerous water resources are exhausted in the middle reaches of the Heihe River Basin in China.

https://doi.org/10.5194/hess-2020-161
Preprint. Discussion started: 4 May 2020

Surface energy balance algorithm for land (SEBAL) model (Bastiaanssen et al., 1998a and 1998b) is currently a crucial method for estimating water and heat fluxes. Using remote sensing data and meteorology knowledge, calculating water and heat fluxes on a daily scale is feasible and widely applied (Bastiaanssen et al., 2000; Teixeira et al., 2009; Liu, 2008; Yin, 2014; Li et al.,, 2010; Ahmad et al.,,2014; Usman et al., 2015) . Liu (2008) verified that the SEBAL model is sensitive to daily global solar radiation (GSR). Therefore, the daily GSR is an important input parameter for ET estimation using the SEBAL model.

The solar radiation that reaches the ground is affected by astronomical, atmospheric (i.e., air molecules, water vapor, and cloud), and surface factors (i.e., slope, aspect, terrain shading, and surface coverage). Thus, the simulation of GSR in a rugged terrain is significantly complex (Zeng et al., 2005; Yeom et al., 2016; Shi et al., 2018). Geographical information system (GIS) and remote sensing techniques have provided new methods for estimating solar radiation, including the above mentioned factors. Digital elevation model (DEM) data have been extensively used to simulate solar radiation in mountainous areas (Williams et al., 1972; Bocquet, 1984; Dozier and Frew, 1990; Qiu et al., 2003; Chen et al., 2013; Shi et al., 2018). However, research on the daily GSR is limited to accurately estimating climate factors on a daily scale. Chen et al., (2013) developed a DEM-based radiation model to estimate instantaneous clear-sky solar radiation for surface energy balance system to obtain accurate energy absorbed by the mountain surface. However, terrain shading is insufficiently considered. Shi et al., (2018) used Iqbal model C (1983) and DEM to

https://doi.org/10.5194/hess-2020-161
Preprint. Discussion started: 4 May 2020

Hydrology and Earth System Sciences
Open Access
Discussions

estimate the daily GSR to investigate the effects of topography. The daily GSR was acquired in a relatively coarse grid of 1 km×1 km. However, their method was not applied to a high spatiotemporal resolution estimation of the GSR directly, thereby making the performance of agriculture activities infeasible.

In the present study, a distributed model for daily GSR is proposed on the basis of possible solar radiation, which includes astronomical, atmospheric, and land surface factors in a relatively high spatiotemporal resolution. Based on the DEM data with 100 m resolution, weather station information (radiation, wind, and pressure), and remote sensing images of thematic mapper (TM) and moderate-resolution imaging spectroradiometer (MODIS), this study aims to 1) realize the estimation of daily GSR in a 100 m×100 m resolution, 2) compare and validate the estimated results with measured data, and 3) improve the application of simulated daily GSR by calculating ET using the SEBAL model.

2. Methodology

2.1. Study Area

The study area is located in the middle reaches of the Heihe River Basin in Northwestern China, including Linze County and Ganzhou District, with an elevation range of 1,360–3,600 m and an area of approximately 60,000 km2 (Fig. 1). An oasis is situated along the river, surrounded by a desert (Fig. 2). This area is typical warm temperate desert arid climate.

https://doi.org/10.5194/hess-2020-161
Preprint. Discussion started: 4 May 2020

2.2. Data

2.2.1. Remote sensing data

Landsat TM data can provide high-resolution information about land surface temperature, land cover classification, albedo, normalized difference vegetation index(NDVI), and emissivity. This study adopts the Landsat TM5 image that was captured on June 24, 2009, in which the cloud cover in the study area was below 5% due to a favorable weather condition (Fig. 5a).

MODIS Levels 2 and 3 images on June 21–24, 2009, without clouds are collected. NDVI, emissivity, and surface albedo are retrieved by using Level 2 products (500 m×500 m). Daily land surface temperature (LST) with a spatial resolution of 1 km comes from Level 3 MOD11A1.

2.2.2. Meteorological data

To supplement the TM and MODIS images, the heights of vegetation and the following meteorological data are required: air pressure, relative humidity, air temperature, sunshine duration, LST, wind speed, net radiation, and daily GSR. In addition, two ET measurements are placed in a farmland and a wetland station (Fig. 1). All the meteorological data must be measured hourly throughout the day.

2.2.3. GIS data

Considering the spatiotemporal resolution of remote sensing data, this study uses the DEM with a spatial resolution of 100 m×100 m and the vector map of the administrative boundary with the map scale of 1:250,000. All data are obtained from

https://doi.org/10.5194/hess-2020-161
Preprint. Discussion started: 4 May 2020

Hydrology and Earth System Sciences Discussions
Open Access
EGU

the website of Digital Heihe (http://heihe.westgis.ac.cn). The land cover map is created by a computer-assisted visual interpretation at the scale of 1:100,000 on the basis of the TM image (Fig. 2).

2.3. Methodology

2.3.1. Improved daily GSR model

The daily GSR in the SEBAL model is calculated as follows (Bastiaanssen et al., 1998a and 1998b; Chen et al., 2000):

$$R_{a24} = G_{sc} \times d_r \times \int_{\omega_1}^{\omega_2} \cos\theta d\omega, \quad (1)$$

where R_{a24} is the daily GSR, G_{sc} is the solar constant, that is, 1367W/m^2, d_r is the earth-sun distance factor (dimensionless), ω_1 and ω_2 represent the solar hour angles (radians) at 5 min after sunrise and at 5 min before sunset, respectively, and θ is the solar zenith angle. $\cos\theta$ is calculated by Chen et al., method(2013).

In Eq. (1), only sun–earth spatial relations on a specific date, slope, and aspect relations are considered. The effects of wet–clean air conditions and the terrain shading are disregarded. The improved daily GSR model includes the above mentioned factors, which can be categorized into two main models.

(1) Determination of GSR over a horizontal surface

The effects of air molecules, O_3, CO_2, oxygen, and other mixed gas and water vapor on short-wave solar radiation are considered in this part by using Iqbal Model C. A detailed description is presented in Shi et al., method (2018).

We obtain the daily global radiation under wet–clean air conditions using

$$Q_{0w} = \frac{T}{2\pi} \int_{-\omega_0}^{\omega_0} I_t d\omega, \quad (2)$$

https://doi.org/10.5194/hess-2020-161
Preprint. Discussion started: 4 May 2020

where $-\omega_0$ and ω_0 represent the solar hour angles at sunrise and sunset, T is the length of a day, and I_t is global irradiance.

(2) Determination of GSR over rugged terrains

The effects of aerosol, land surface factors (slope, aspect, terrain shading, and surface cover), and cloud are considered in this part.

The daily GSR received on land surface consists of three parts (Fu, 1983).

$$Q_{\alpha\beta} = Q_{b\alpha\beta} + Q_{d\alpha\beta} + Q_{r\alpha\beta}, \quad (3)$$

where $Q_{\alpha\beta}$ is the daily GSR over rugged terrains, $Q_{b\alpha\beta}$ is the daily direct solar radiation over rugged terrains, $Q_{d\alpha\beta}$ is the daily diffuse solar radiation over rugged terrains, and $Q_{r\alpha\beta}$ is the daily reflected solar radiation over rugged terrains.

To determine $Q_{b\alpha\beta}$, we assume that

$$Q_{b\alpha\beta} = \frac{Q_{0\alpha\beta}}{Q_{0w}} Q_b = R_b Q_b, \quad (4)$$

$$Q_{b\alpha\beta} = Q_{0\alpha\beta} \frac{Q_b}{Q_{0w}} = Q_{0\alpha\beta} \frac{Q_b}{Q} \frac{Q}{Q_{0w}} = Q_{0\alpha\beta} f_b k_t, \quad (5)$$

where $Q_{0\alpha\beta}$ and Q_{0w} are the daily astronomical solar radiation over a terrain and a horizontal surface, correspondingly, and Q_b is the direct solar radiation over a horizontal surface. R_b represents the effects of slope, aspect, and topographic shadow, Q is the daily GSR over a horizontal surface, f_b is the direct component coefficient, and $k_t = a_G + b_G s$ (where s is the percentage of sunshine duration, and a_G and b_G are empirical coefficients) is the clear sky coefficient. The effects of aerosol and cloud are considered in the term $a_G + b_G s$.

Similar to Eq. (5), we derive an expression for the diffuse component.

$$Q_{d\alpha\beta} = Q_d [f_b k_t R_b + V(1 - f_b k_t)], \quad (6)$$

https://doi.org/10.5194/hess-2020-161
Preprint. Discussion started: 4 May 2020

where Q_d is the diffuse solar radiation in the horizontal surface, and V is the terrain openness (terrain openness + terrain shading = 1). The method for determining V is described by Qiu (2003).

$Q_{0\alpha\beta}$ is calculated using Qiu's (2003) model, and Q_b and Q_d are calculated on the basis of the empirical model exhibited by daily direct solar radiation and diffuse solar radiation in the radiation station considering the effects of aerosol and cloud.

Finally, the reflected radiation from the sloped surface can be computed by the following expressions:

$$\begin{cases} Q_{r\alpha\beta} = Q\rho_g(1-V) & V <=1 \\ Q_{r\alpha\beta} = 0 & V > 1 \end{cases}, \qquad (7)$$

where ρ_g is the surface albedo, which can be retrieved from Landsat TM5 and MODIS09GA. ρ_g is described in detail in Appendix.

2.3.2. SEBAL model principle

The SEBAL procedure consists of a series of algorithms. In this study, this procedure is implemented using the ModelMaker module of ERDAS software. The algorithms solve the complete energy balance equation

$$\lambda ET = R_n - G - H, \qquad (8)$$

where λET is the latent heat flux, R_n is the surface net radiation flux, G is the oil heat flux, and H is the sensible heat flux.

The parameterization of R_n and G is mature. Thus, the core issue of the model is calculating H and ET. SEBAL model introduces a Monin-Obukhov loop iteration to estimate H.

https://doi.org/10.5194/hess-2020-161
Preprint. Discussion started: 4 May 2020

The above mentioned instantaneous results (H , R_n ,and G_0) are substituted in the energy balance Eq. (8) to calculate instantaneous latent heat flux λET . The daily time scaling extension of the model is implemented on the basis of the evaporative fraction (EF) method.

$$\frac{\lambda ET}{R_n - G} = EF, \tag{9}$$

Following Shuttleworth et al., (1989), the instantaneous EF is assumed to be similar to its 24 h counterpart (Brutsaert et al., 1992; Crago, 1996) and the assumption supported by numerous field studies (Bastiaanssen et al., 1998a, b; Morse et al., 2000).

Soil heat flux for 24 h periods is assumed to be nearly 0 for vegetated surfaces given the canceling effect of positive G during daylight and negative G during nighttime. Therefore, an actual λET_{24} for the 24-h evaporation can be computed as

$$\lambda ET_{24} = EF \times R_{n24}, \tag{10}$$

where R_{n24} is the daily net radiation. The accuracy of the daily GSR estimation largely determines the accuracy of R_{n24} estimation.

2.3.3. Combination of multi-source remote sensing data for ET simulation

Liu (2008) conducted a sensitivity analysis of the SEBAL model and suggested that the LST and emissivity are highly sensitive to the simulated ET, whereas the surface albedo, wind speed, NDVI, and aerodynamic roughness of a surface are slightly sensitive to ET.

Only MODIS data can be used to calculate the daily ET because no TM data

https://doi.org/10.5194/hess-2020-161
Preprint. Discussion started: 4 May 2020

from June 21 to 23, 2009, are available. Therefore, a co-simulation experiment on the ET simulation, which uses three strategies of land surface parameters, is performed in the present study. TM strategy refers to all the land surface parameters retrieved by the TM image. MODIS strategy refers to all the land surface parameters retrieved by the MODIS image. The TM/MODIS hybrid strategy, which combines the advantages of the first two methods, refers to the LST from the MODIS11A1 image and the surface albedo and NDVI from the TM image. The addition of the TM surface albedo and NDVI can improve spatial resolution, whereas adding the MODIS LST can improve temporal resolution. We can approximate that no change will occur in the surface albedo and NDVI within a few days.

The TM image cycle is 16 days with a high spatial resolution, whereas the MODIS image cycle is 1 day. However, the spatial resolution is less than the TM image. Many local features retrieved by the TM image are generalized in the image retrieved by MODIS. The TM/MODIS hybrid combines the advantages of the spatiotemporal resolution of both strategies.

3. Results and discussion

3.1. Daily GSR

3.1.1. Accuracy of simulated result

The validation results of the two models are summarized in Table 1. The mean absolute bias error (MABE) of the improved daily GSR model is 9 W/m^2, and the mean absolute relative bias error (MARBE) is 2.5%. The MABE of the daily GSR in

https://doi.org/10.5194/hess-2020-161
Preprint. Discussion started: 4 May 2020

the SEBAL model is 122.2 W/m^2, and the MARBE is 33.9%.

The results show that the GSR on June 24, 2009, calculated in the SEBAL model ranged from 438 W/m^2 to 465.7 W/m^2 with a mean of 446 W/m^2, which was much higher than the improved daily GSR model with a range of 350–394 W/m^2 and a mean of 370 W/m^2.

In Eq. (7), the surface albedo is calculated by two remote sensing data. The result indicates that a slight difference of 0.4 W/m^2 in the daily GSR emerges by using the surface albedo from the TM and MODIS images on June 24, 2009.

3.1.2. Spatial pattern of daily GSR

Theoretically, the GSR is larger on a sunny slope (an open place) than on a shady slope (a rugged place), thereby indicating that the daily GSR is large where the sunshine duration is long.

The spatial distribution of the daily GSR calculated using the SEBAL model presents discontinuous and improper stripes (Fig. 3a). However, the calculation of the improved model is more reasonable, because the effects of the spatial position relations, percentage of sunshine, slope, aspect, terrain shading, and atmospheric influence are comprehensively reflected.

An obvious difference between the SEBAL and the improved models is observed in the southern area and the Longshou Mountain (Fig. 3b). The daily GSR in the SEBAL model has reached the maximum value in the two areas. However, the daily GSR in the improved model is near the minimal value. This result can be attributed to the terrain shading that included a diffuse and reflected solar radiation in the new

https://doi.org/10.5194/hess-2020-161
Preprint. Discussion started: 4 May 2020

model. In addition, the percentage of sunshine is higher in the northwest, thus implying that sunshine duration is long, and the corresponding daily GSR is high (Fig. 3b). However, these distribution features are unclear in the daily GSR in the SEBAL model.

The daily GSR of 0 °, 45 °, 90 °, and 360 ° in the slope direction of the study area are statistically analyzed, and then the mean value is calculated (Fig. 4). In terms of local surface distribution pattern, the daily GSR must reach the maximum value near the south slope at 180 °. However, the simulated results using the SEBAL model show that the daily GSR is only the minimum value (Fig. 4a), and the error is corrected by the improved model (Fig. 4b).

Therefore, the improved daily GSR model improves the calculation accuracy and makes the spatial distribution more reasonable than the original model.

3.2. Daily ET

3.2.1. Accuracy of simulated Daily ET

The comparative analysis of oasis stations (farmland [plain area]) is listed in Tables 2 and 3. The accuracy of the daily ET is higher in the improved scheme than in the original scheme, and ET is near the measured ET. The results show that the improved scheme using the TM/MODIS hybrid strategy is the optimum among the three models.

The simulated ET analysis of the TM/MODIS hybrid strategy of oasis stations from June 21 to 24, 2009, is summarized in Table 4. The mean measured ET for 4 days was 4.8 mm. The MABE of the improved scheme-simulated ET is 0.6 mm, and

https://doi.org/10.5194/hess-2020-161
Preprint. Discussion started: 4 May 2020

the MARBE is 12%. For the original scheme ET, the MABE is 1.85 mm, and the MARBE is 39%. The mean ET of the wetland station (saline land) in 4 days is 2.2 mm. The simulated ET changes from 3.5 mm (original scheme) to 2.2 mm (improved scheme).

According to the research purpose and China's land use classification system, the study area is divided into 22 underlying surface coverage types (Fig. 2). Therefore, the TM/MODIS hybrid strategy of the original and improved schemes are used to calculate the ET of the 23rd and 24th days, respectively. The mean ETs of the two days in each surface coverage type are calculated and listed in Table 5. The mean measured ET for the two days is 4.6 mm in the farmland station. It changes from 6.3 mm (original scheme) to 4.3 mm (improved scheme). The mean measured ET for the two days is 2.2 mm in the wetland station. It changes from 3.7 mm (original scheme) to 2.4 mm (improved scheme).

In Table 5, the highest ET value has appeared in all types of water bodies, followed by farmland, forest, wetland, and residential areas. The ET values in the Gobi Desert and bare rock land are low. The water consumption in these areas is dominated by agriculture. The mean daily water consumption in the study area is 1.46×10^7 m^3. The farmland, which accounts for 44.8%, has consumed 6.5×10^6 m^3 in the improved scheme, and 9.5×10^6 m^3 in the original scheme.

3.2.2. Spatial pattern of daily ET

Figs. 5 and 6 illustrate that, for all land cover types, except for water bodies, the highest ET value is found over the farmland given the presence of irrigation water. In addition, the ET is low in the area around the oasis. The differences in ET over the various land types mainly depends on the NDVI. A large NDVI value indicates a high ET.

In Fig. 5 and 6, the simulation ET based on the improved scheme declines more than the original scheme. In the improved scheme, the desert ET is mainly distributed in the vicinity of 0 mm, and the oasis ET is in the vicinity of 4.8 mm. In the original scheme, the desert ET is mainly distributed in the vicinity of 0 mm, and the oasis ET is in the vicinity of 6.5 mm.

The TM strategy has the highest resolution (Figs. 5a and 6a), whereas the MODIS strategy has the lowest (Fig. 5b and 6b); many features retrieved by the TM strategy are generalized in the image. The TM/MODIS hybrid strategy (Fig. 5c and 6c) combines the advantages of the spatiotemporal resolution of both strategies to provide a feasible scheme for the estimation of the daily ET on improving temporal resolution and maintaining a relatively detailed spatial resolution.

Figs. 5a and 6a are images with cloud and cloud shadows at the northwest corner, correspondingly. Several parts of the LST image in Figs. 5b and 6b are missing; this phenomenon mostly occurs in desert areas. These areas are smaller than the entire study area and cannot affect the statistical characteristics of various types of land ET.

4. Conclusions

The new model fully considers the atmospheric and surface factors, especially

https://doi.org/10.5194/hess-2020-161
Preprint. Discussion started: 4 May 2020

the influence of terrain shading on diffuse solar radiation and reflected solar radiation over rugged terrains.

In order to estimate daily ET accurately, a new method for estimating the daily GSR over the rugged terrains in the middle reaches of the Heihe River Basin is proposed in this study. This method is based on Iqbal model C, fully considering the atmospheric and surface factors, especially the influence of terrain shading on diffuse solar radiation and reflected solar radiation over rugged terrains. The daily surface ET on June 21–24, 2009, is simulated by using the SEBAL model, and a portion of the daily GSR in the SEBAL model is improved. The results can be summarized as follows:

The improved daily GSR with a resolution of 100 m×100 m is implemented; the MABE of the simulated results is 9 W/m^2, and the MARBE is 2.5%. The MABE of the daily GSR in the SEBAL model is 122.2 W/m^2, and the MARBE is 33.9%.

Theoretically, the spatial distribution of the daily GSR is more reasonable using the improved model than the original model. The GSR is larger on a sunny slope (an open place) than on a shady slope (a rugged place). In addition, if the percentage of sunshine in the northwest is high, then the daily GSR is also high. The estimated result of the improved daily GSR model is consistent with the distribution law, but the estimated result of the SEBAL daily GSR model cannot fully reflect.

The co-simulation experiment on the ET simulation is designed for three strategies, namely, TM, MODIS, and TM/MODIS hybrid strategies. They are used in the original SEBAL model (original scheme) and the improved daily GSR SEBAL model (improved scheme). The results show that the improved scheme ET is more accurate than the original scheme. Moreover, the TM/MODIS hybrid strategy in the improved scheme is the most reasonable in terms of accuracy and spatial distribution.

The simulated ET declines more based on the improved scheme than based on the original scheme. The mean measured ET of the oasis station in 4 days is 4.8 mm. The original scheme ET is 6.9 mm, and the improved scheme ET is 4.2 mm using the TM/MODIS hybrid strategy. The MABE of ET decreases from 2.1 mm (original scheme) to 0.6 mm (improved scheme), and the MARBE declines from 44% to 13% accordingly. And in all schemes desert ET is mainly distributed in the vicinity of 0 mm.

All simulated ETs show that the highest ET value is found in farmland, except for water bodies considering the presence of irrigation water, followed by farmland, forest, wetland, and residential areas, the lowest values appeared over bare rock land.

Different combination strategies show that the TM strategy has the highest resolution, and the MODIS strategy has the lowest; however, the TM image cycle is 16 days, whereas the MODIS image cycle is 1 day. The TM/MODIS hybrid strategy combines the advantages of the spatiotemporal resolution of both strategies.

During the growing season, the surface albedo and the height of the vegetation change daily. The calculation of ET is influenced by the satellite image quality, and the clouding images cannot be used. Thus, simulating continuously is difficult, especially using the TM/MODIS hybrid scheme. An approach that combines the ET estimates obtained from the TM with the drainage lysimeters has been verified useful

https://doi.org/10.5194/hess-2020-161
Preprint. Discussion started: 4 May 2020

in computing cumulative ET (Morse et al., 2000).

In the growing season, the water of Heihe River is mainly consumed in the middle reaches. Therefore, accurate calculation of water consumption of various land types in the middle reaches, especially agricultural production, can effectively use limited water resources, leave more water to the downstream, and make the downstream ecological environment better.

Appendix

MODIS09GA

Broadband shortwave surface albedo is calculated from the normalized reflection values of Channels 1, 2, 3, 4, 5, and 7 using the following equation (Liang et al., 2003):

$$\rho_g = 0.160\alpha_1 + 0.291\alpha_2 + 0.243\alpha_3 + 0.116\alpha_4 + 0.112\alpha_5 + 0.081\alpha_7 - 0.0015. \quad (1)$$

TM5

$$\rho_g = \frac{\alpha_{toa} - \alpha_{path\_radiance}}{\tau_{sw}^{2}}, \quad (2)$$

where α_{toa} is the atmospheric top reflectivity and can be obtained from the weighted average of the reflectivity of the shortwave bands (1, 2, 3, 4, 5, and 7 bands of TM) in remote sensing images. $\alpha_{path\_radiance}$ is the albedo path radiance, and τ_{sw}^{2} is the two-way transmittance (Morse et al., 2000).

Data availability. Meteorological data are available from the authors by request. DEM and vector map of the boundary were provided by Digital Heihe (http://heihe.westgis.ac.cn). Remote sensing data are available from https://ladsweb.modaps.eosdis.nasa.gov/ and http://www.gscloud.cn/sources/?cdataid=263&pdataid=10

Author contributions. Prof. Qiu and Liu give theoretical guidance, Doc. Li gives technical guidance and data support, Doc. Shi gives help in daily GSR calculation.

Competing interests. The authors declare that they have no conflict of interest.

Acknowledgements. We are grateful to Prof. Yang Xin of the Nanjing Normal University for her useful suggestions. This research was supported by China NSF (Nos. 41971382, 41301036, 41871285, 41771415, and 41805083).

Financial support. This research has been supported by China NSF (Nos. 41971382, 41301036, 41871285, 41771415, and 41805083).

References

Teixeira AH de C, Bastiaanssen WGM, Ahmad MD, Bos MG: Reviewing SEBAL input parameters for assessing evapotranspiration and water productivity for the Low-Middle Sao Francisco River basin, Brazil Part A: Calibration and validation. Agr Forest Meteorol 149,462-476. https://doi.org/10.1016/j.agrformet.2008.09.016,2009

Bastiaanssen WGM, Menenti M, Feddes RA, Holtslag AAM:The Surface Energy Balance Algorithm for Land (SEBAL): Part 1 formulation, Journal of Hydrology 212-213: 198-212, 1998a.

Bastiaanssen WGM, Pelgrum H, Wang J, Ma Y, Moreno J, Roerink GJand van der Wal T : A remote sensing Surface Energy Balance Algorithm for Land (SEBAL): Part 2 validation. J. Hydr. 212-213,213-229,(1998b.

https://doi.org/10.5194/hess-2020-161
Preprint. Discussion started: 4 May 2020

Hydrology and Earth System Sciences
Open Access
Discussions

Bastiaanssen WGM, Noordman EJM,Pelgrum H,Davids G,Thoreson BP,Allen RG: SEBAL model with remotely sensed data to improve water-resources management under actual field conditions. J. Irrig. Drain. Eng. 131(1), 85-93,2005.

Brutsaert W, Sugita M:Application of Self-Preservation in the Diurnal Evolution of the Surface Energy Budget to Determine Daily Evaporation. J. Geophys. Res. 97, 18377-18382. http://dx.doi.org/10.1029/92JD00255, 1992.

Crago RD: Conservation and variability of the evaporative fraction during the daytime.J.Hydrol.,180,173-194,1996.

Fu B P:Mountain Climate. Beijing Science Press 270 pp,1983.

Iqbal M:An Introduction to Solar Radiation. Academic Press 390 pp, 1983.

Kite GW: Using a basin-scale hydrological model to estimate crop transpiration and soil evaporation. J. Hydr 229:59-69,2000.

Li SB, Zhao WZ: Satellite-based actual evapotranspiration estimation in the middle reach of the Heihe River Basin using the SEBAL method. Hydrol. Process 24, 3337-3344. doi: 10.1002/hyp.7748,2000.

Liang S, Shuey CJ, Russ AL,et al.: Narrowband to broadband conversions of land surface albedo.J. Ⅱ-Validation. Remote Sens. Environ 84(l):25- 41,2000.

Liu CS Regional Land Surface Water/Heat Flux Modeling and Application Based on Remote Sensing in Shandong Province. Phd. thesis, Nanjing University of Information Science & Technology, 2008.

Markham B, Barker J: Landsat MSS and TM post-calibration dynamic ranges, exo-atmospheric reflectances and at-satellite temperatures. Landsat Technical Notes, 1986.

Mobin-ud Din Ahmad, Mac Kirby, Mohammad Shahidul Islam,et al.: Groundwater Use for Irrigation and its Productivity: Status and Opportunities for Crop Intensification for Food Security in Bangladesh. Water Resour Manag 28(5), 1415-1429.doi: 10.1007/s11269-014-0560-z, 2014.

Morse A, Tasumi M, Allen RG, Kramber WJ:Application of the SEBAL methodology for estimating consumptive use of water and streamflow depletion in the Bear River Basin of Idaho through Remote Sensing. Final Report Submitted to The Raytheon Systems Company Earth Observation System Data and Information System Project, 2000.

Usman M, Liedl R, Awan UK: Spatio-temporal estimation of consumptive water use for assessment of irrigation system performance and management of water resources in irrigated Indus Basin. Pakistan. J. Hydrol 525,26–41. https://doi.org/10.1016/j.jhydrol.2015.03.031, 2015.

Nie ZL: Study on Groundwater Circulation and Renewability in the Middle Reaehes of Heihe River Valley,Northwest China. Phd. thesis, Chinese Academy of Geological Sciences,2004.

Qiu XF: Distributed Modeling of Solar Radiation Over Rugged Terrains. Phd. thesis, Nanjing University, 2003.

Rahman M, Sulis M, Kollet SJ: Evaluating the dual-boundary forcing concept in subsurface–land surface interactions of the hydrological cycle. Hydrol. Process 30,1563-1573. https://doi.org/10.1002/hyp.10702,2016.

Sellers PJ, Randall DA, Collatz CJ, et al.: A revised land surface parameterization (SiB2) for atmosphere GCMs. Part I: Model formulation. J Climate 9: 676-705, 1996.

Shuttleworth WJ, Gurney RJ, Hsu AY, Ormsby JP: FIFE:The variation in energy partition at surface flux sites. In A.Rango(Ed.),Remote sensing and large-scale processes (Proceeding of the IAHS third internation Assembly,Baltimore,MD,May,1989). IAHS Publication,vol.186.(pp.66-74) ,1989.

Shi GP,Qiu XF,Zeng Y: New Method for Estimating Daily Global Solar Radiation over Sloped Topography in China. Adv. Atmos. Sci 35(3), 285 – 295.https://doi.org/10.1007/s00376-017-6243-y,2018.

Chen X, Su Z, Ma Y, Yang K, Wang B: Estimation of surface energy fluxes under complex terrain of Mt. Qomolangma over the Tibetan Plateau. Hydrol. Earth Syst. Sci 17, 1607–1618. doi:10.5194/hess-17-1607-2013,2013

Yin JQ: Study on daily evapotranspiration estimation model by remote sensing coupling daily global solar radiation model and daily mean LST model. Phd. thesis, Nanjing University of Information Science & Technology ,2014.

Yin JQ, Qiu XF, He YJ: Modelling the spatial and temporal variation laws of Diffuse Solar Radiation of Rugged Terrain over Zhejiang Province. Transcations of Atmospheric Sciences 34(1),93-98,2011.

Yeom J M, Seo Y K, Kim D S, Han KS: Solar radiation received by slopes using COMS imagery, a physically based radiation model, and GLOBE. J.Sensors 2016, 4834579, https://doi.org/10.1155/2016/4834579,2016.

Zeng Y,Qiu XF, Liu SM: Distributed modeling of extraterrestrial solar radiation over rugged terrains. Chin J. Geophys-ch 48(5), 1028-1033,2005.

https://doi.org/10.5194/hess-2020-161
Preprint. Discussion started: 4 May 2020

Hydrology and Earth System Sciences
Open Access
Discussions

Figures

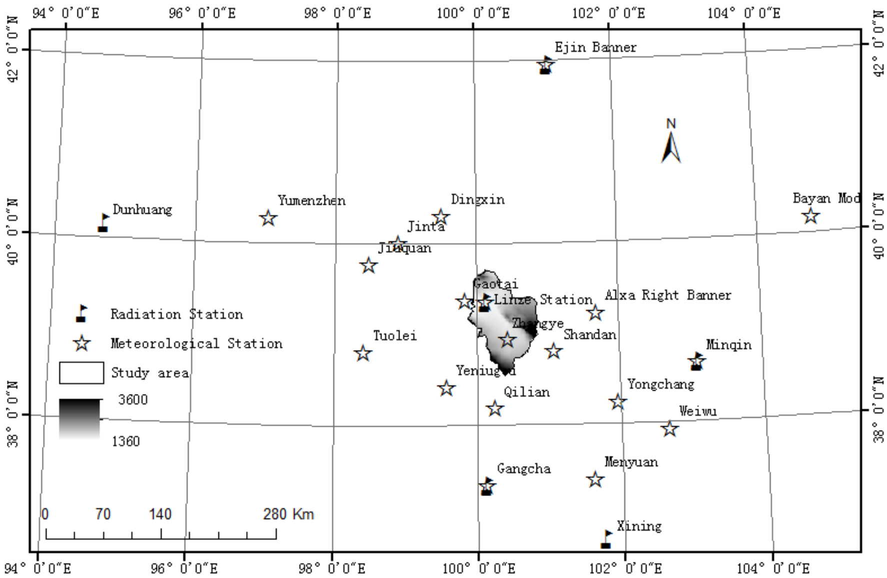

Fig.1. Distribution of meteorological stations and DEM of the middle reach of the Heihe River (unit: m)

https://doi.org/10.5194/hess-2020-161
Preprint. Discussion started: 4 May 2020

Hydrology and Earth System Sciences
Open Access
Discussions

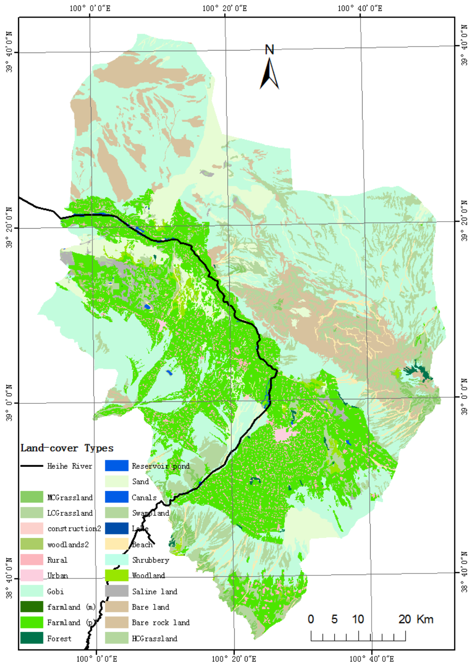

Fig.2. Land-cover map of the study area

(High-coverage grassland: HCGrassland, Moderate-coverage grassland: MCGrassland, Low-coverage grassland: LCGrassland, Sand desert: Sand, Gobi desert: Gobi, Other woodlands:woodlands2, Other construction:construction2, Rural residential: Rural, farmland (mountain):Farmland (m), Farmland (plain):Farmland(P))

https://doi.org/10.5194/hess-2020-161
Preprint. Discussion started: 4 May 2020

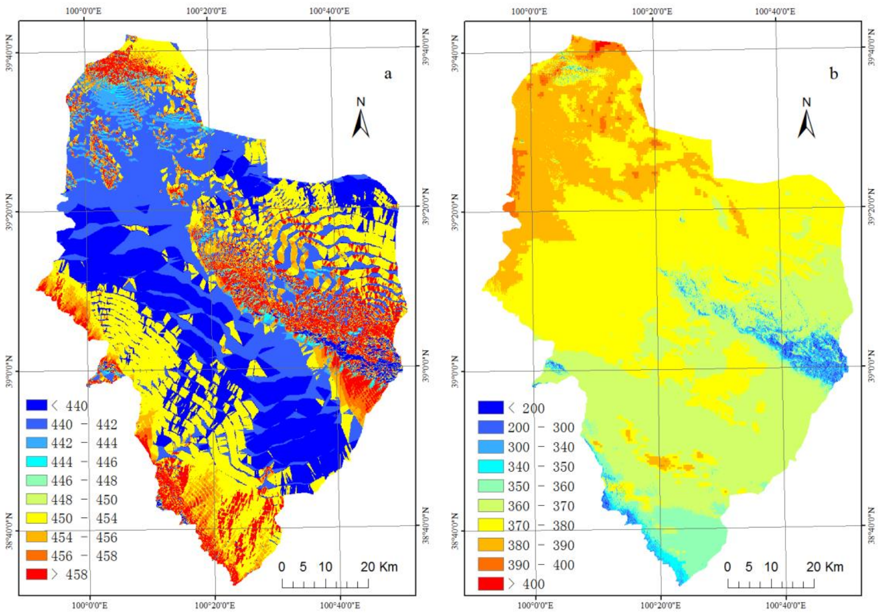

a.original SEBAL model b.improved model

Fig.3. Spatial distribution of daily GSR in the middle Heihe River Basin on 24 June, 2009 (Unit: W/m^2)

https://doi.org/10.5194/hess-2020-161
Preprint. Discussion started: 4 May 2020

Hydrology and Earth System Sciences
Discussions

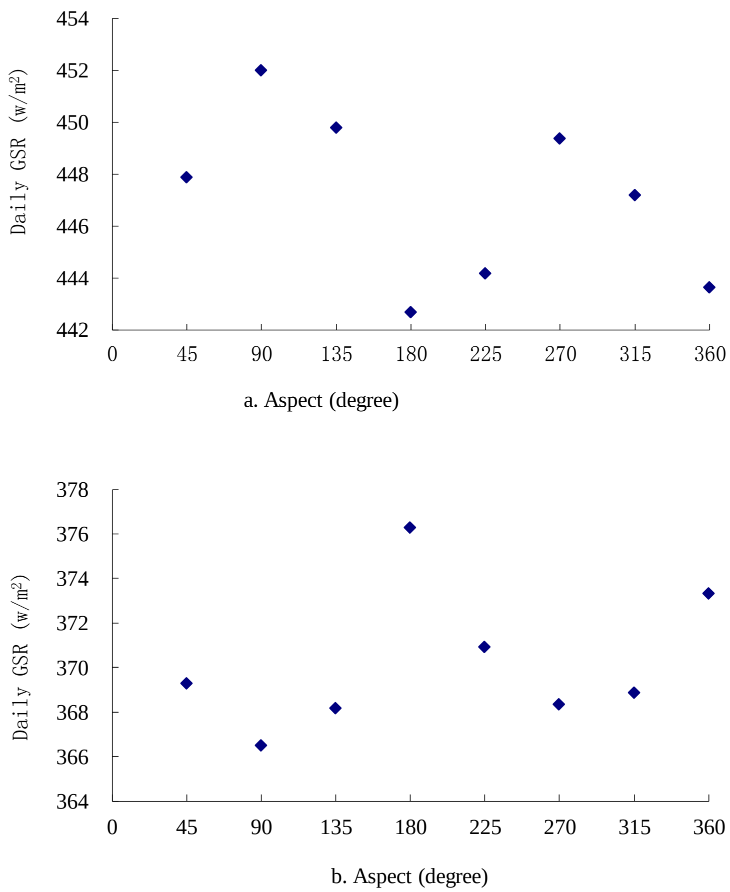

Fig.4. Relation between daily GSR and aspect in the middle Heihe River Basin on 24 June, 2009 (Unit: mm)

(a. original SEBAL model, b. improved model)

https://doi.org/10.5194/hess-2020-161
Preprint. Discussion started: 4 May 2020

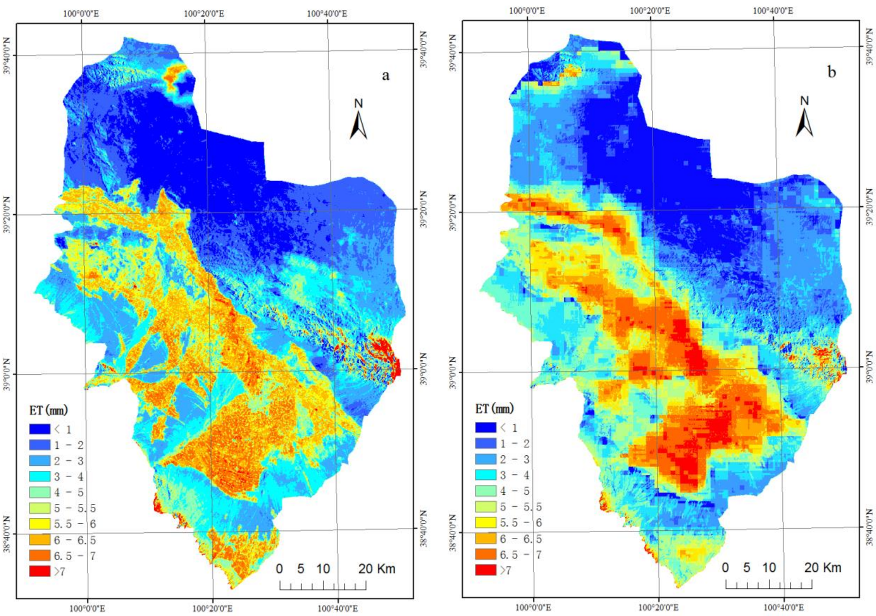

a. TM strategy b. MODIS strategy

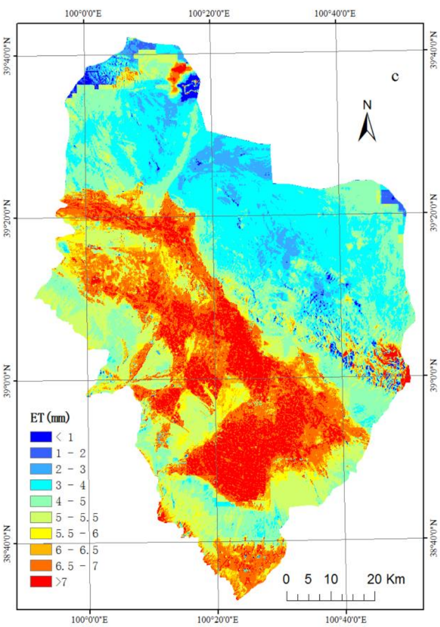

c. TM/MODIS hybrid strategy

Fig.5. Spatial distribution of ET retrieved using original scheme on 24 June, 2009 (Unit: mm)

https://doi.org/10.5194/hess-2020-161
Preprint. Discussion started: 4 May 2020

Hydrology and Earth System Sciences
Open Access
EGU
Discussions

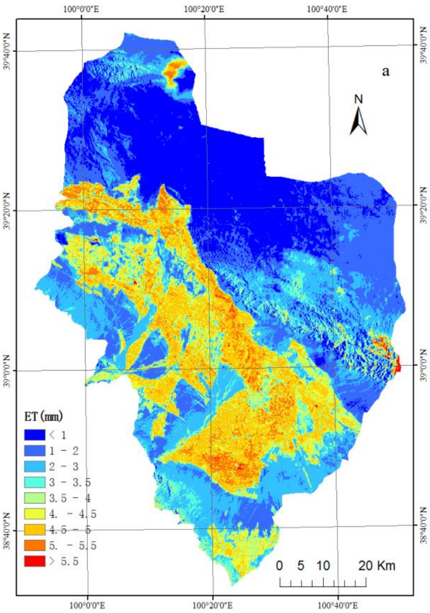

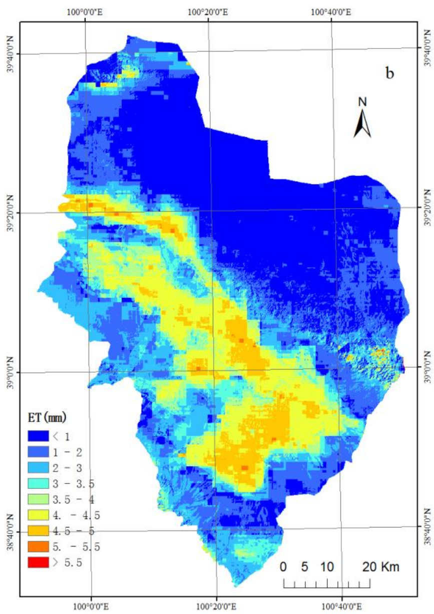

a. TM strategy b. MODIS strategy

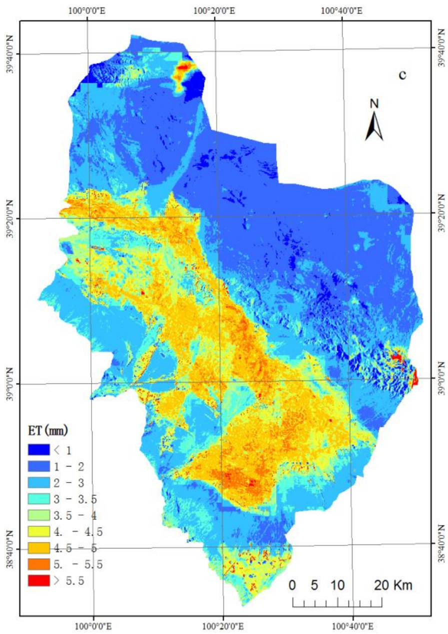

c. TM/MODIS hybrid strategy

Fig.6. Spatial distribution of ET retrieved using improved scheme on 24 June, 2009 (Unit: mm)

https://doi.org/10.5194/hess-2020-161
Preprint. Discussion started: 4 May 2020

Hydrology and Earth System Sciences
Discussions

Tables

Table 1

Daily GSR of middle Heihe River Basin on June 21–24, 2009 (Unit: W/m^2)

Date	measure daily GSR	simulated daily GSR		MABE		MARBE（%）	
		improved	original	improved	original	improved	original
6.21	354.2	346.1	484	8.1	129.8	2.3	36.6
6.22	360	355.3	484.1	4.7	124.1	1.3	34.5
6.23	377.3	375	484.3	2.3	107	0.6	28.4
6.24	356.5	377.3	484.4	20.8	127.9	5.8	35.9
Mean	362	363.4	484.2	9	122.2	2.5	33.9

https://doi.org/10.5194/hess-2020-161
Preprint. Discussion started: 4 May 2020

Hydrology and Earth System Sciences Discussions
Open Access
EGU

Table 2

ET of three combination schemes on 24 June, 2009(Unit: mm)

Classification	measured ET	original scheme	improved scheme
TM strategy	4.8	6.3	5.0
MODIS strategy	4.8	6.3	4.2
TM/MODIS Hybrid strategy	4.8	7.0	4.8

https://doi.org/10.5194/hess-2020-161
Preprint. Discussion started: 4 May 2020

Table 3

Errors of ETs of three combination strategies on 24 June, 2009(Unit: mm)

simulation strategy	simulation scheme	MABE	MABRE (%)
TM strategy	original scheme	1.5	31
	improved scheme	0.2	4
MODIS strategy	original scheme	1.5	31
	improved scheme	0.6	13
TM/MODIS strategy	original scheme	2.2	46
	improved scheme	0	0

https://doi.org/10.5194/hess-2020-161
Preprint. Discussion started: 4 May 2020

Hydrology and Earth System Sciences
Discussions
Open Access

Table 4
Daily ET of middle Heihe River Basin on June 21–24, 2009 (Unit: mm)

Date	Measure ET	simulated ET		MABE		MARBE（%）	
		improved	original	improved	original	improved	original
6.21	4.9	3.8	6.6	1.1	1.7	22	35
6.22	5.1	3.9	6.5	1.2	1.4	24	27
6.23	4.5	4.4	6.6	0.1	2.1	2	47
6.24	4.8	4.8	7	0	2.2	0	46
Mean	4.8	4.2	6.7	0.6	1.85	12	39

https://doi.org/10.5194/hess-2020-161
Preprint. Discussion started: 4 May 2020

Hydrology and Earth System Sciences
Open Access
Discussions
EGU

Table 5

ET of each land-cover types

Underlying Surface Type	Area (km^2)	improved scheme Mean ET (mm)	original scheme Mean ET (mm)
Forest land	16.43	3.5	5.6
Shrubbery	15.73	2.1	3.6
Woodland	56.99	3.4	5
Other woodlands	7.89	3.5	5.3
High-coverage grassland	36.43	3	4.9
Moderate-coverage grassland	76.43	2.5	4.2
Low-coverage grassland	731.89	1.9	3
Canals	20.24	4.5	6.6
Lake	0.16	3.6	5.4
Reservoir pond	4.2	4	5.6
Beach	106.18	2.1	3.2
Urban Land	15.33	3.8	5.5
Rural residential land	164.1	4	5.9
Other construction lands	4.51	3.8	5.6
Sand desert	472.64	1.4	2.3
Gobi desert	2321.37	1.4	2.1
Saline land	49.2	2.4	3.7
Swampland	4.48	4.2	6
Bare land	78.74	1.1	1.7
Bare rock land	558.52	1.5	2.3
farmland (mountain area)	0.13	3.7	5.9
Farmland (plain area)	1515.16	4.3	6.3